9

Power Output Characteristics of Transparent a-Si BiPV Window Module

Jongho Yoon
Hanbat National University
Republic of Korea

1. Introduction

Energy-related concerns about traditional resources include the depletion of fossil fuel, a dramatic increase in oil prices, the global warming effect caused by pollutant emissions from conventional energy resources, and the increase in the energy demand. These concerns have resulted in the recent remarkable growth of renewable energy industries [1-3]. Furthermore, renewable energy has become a significantly important research area for many researchers as well as for governments of many countries as they attempt to ensure the safety, long-term capability, and sustainability of the use of global alternative energy resources [2]. Renewable energy resources include solar, geothermal, wind, biomass, ocean, and hydroelectric energy. [4] In particular, both solar (i.e. photovoltaics) and wind energy are considered to be leading technologies with respect to electrical power generation.
The study of photovoltaics (PV) has been carried out since the 1980s' and is currently the most significant renewable energy resources available. According to the Renewable Energy Policy Network for the 21st Century (REN21), there has been a strong growth in the use of PV of 55 % and the worldwide solar PV electric capacity is expected to increase from 1,000 MW in 2000 to 140,000 MW by 2030 [5]. Moreover, it is forecast by the European Renewable Energy Council that this renewable electric energy could become sufficient to cover the base load and half of the global electricity energy demand by 2040 [6]. Generally in the PV industry, crystalline silicon has generally occupied about 95 % of the market share of materials, while only 5 % of all solar cells use amorphous silicon [7]. However, in order to improve the cost efficiency of solar cells by using less material, the thin-film PV module with amorphous silicon has become an active research and development (R&D) area [8]. In particular, solar cells that use amorphous silicon have the advantage of being able to generate a higher energy output under high temperatures than crystalline silicon solar cells, which are less affected by the temperature increase with respect to performance of electricity output than are the crystalline silicon solar cells. Moreover, installed at the rooftop and on the exterior wall of the building, a thin-film solar cell can be conveniently used as a façade that generates power for the entire building. This system is known as a building integrated photovoltaic system (BIPV). The thin-film solar cell can also provide the advantage of heat insulation and shading when incorporated into a harmonious building design. Therefore, the thin-film solar cell is expected to be a very bright prospect as a new engine for economical growth in the near future. Currently in Korea, many researchers are conducting

vigorous research on PV with respect to the application of crystalline silicon solar cells. An example of such research includes the evaluation of the power output of PV modules with respect to the ventilation of the rear side of the module. However, research on the transparent thin-film solar cell as a building façade application including windows and doors is only in its early stages.

Therefore, the objective of this study is to establish building application data for the replacement of conventional building materials with thin-film solar cells. In this study, an evaluation is carried out on the performance of the thin-film solar cell through long-term monitoring of the power output according to the inclined slope (the incidence angle). This is conducted by using a full-scale mock-up model of the thin-film solar cell applied to a double glazed system. In addition, the aim of the application data of the thin-film solar cell is to analyze the effect of both the inclined slope and the azimuth angle on the power output performance by comparing this data with the simulation data for PV modules[9].

2. Methodology

In this study, a full-scale mock-up model was constructed in order to evaluate the power output performance of a PV module laminated with a transparent thin-film solar cell. A mock-up model was designed for a PV module that had a range of inclined slopes, and was used to measure the power output according to the slope (incidence angle) and the azimuth angle. The collected experimental data was then compared with the simulated data for a power performance analysis.

A commercialized single plate transparent thin-film solar cell with amorphous silicon was used in this study (KANEKA, Japan). This was modified into a double glazed PV module in order to install the mock-up model for this study.

Using the full-scale mock-up model, the system output was monitored for 9 months. A computer simulation (TRNSYS, University of Wisconsin, USA) of the PV module was also performed at the same time, and empirical application data was calibrated for the statistical analysis of power performance based on the inclined slope and the azimuth angle. In particular, the annual power output of the PV module was obtained by analyzing the data obtained from the remaining 3 months on the basis of the 30 years' standard weather data in Korea.

3. Double-glazed PV module

In Korea, it is an obligatory requirement that building materials such as windows and doors for a residence should be double glazed in order to ensure adequate heat insulation. Moreover, as the demand for energy efficiency buildings increases, the efficiency of double glazed window systems is improving with respect to heat insulation, as is the efficiency of exterior wall systems of buildings. Therefore, the photovoltaic characteristic of thin-film solar cells was measured in terms of the transmittance of the cell prior to evaluation of the PV module (Figure 1). The results of this measurement showed an average transmittance of 10 % at the range of visible radiation between 390 nm and 750 nm.

Using this thin-film solar cell, a single plate PV module was manufactured to a thickness of 10 mm, and the PV module was then modified as a double glazed module of 27 mm thick, consisting of a 12 mm air space and a 5 mm thick layer of common transparent glass, as shown in Figure 2.

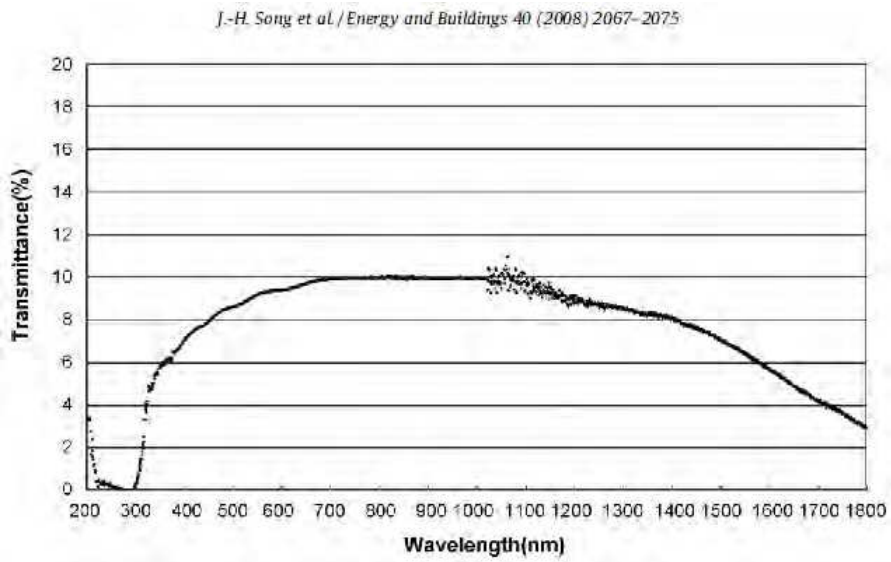

Fig. 1. Transmittance of PV module depending on the wavelength

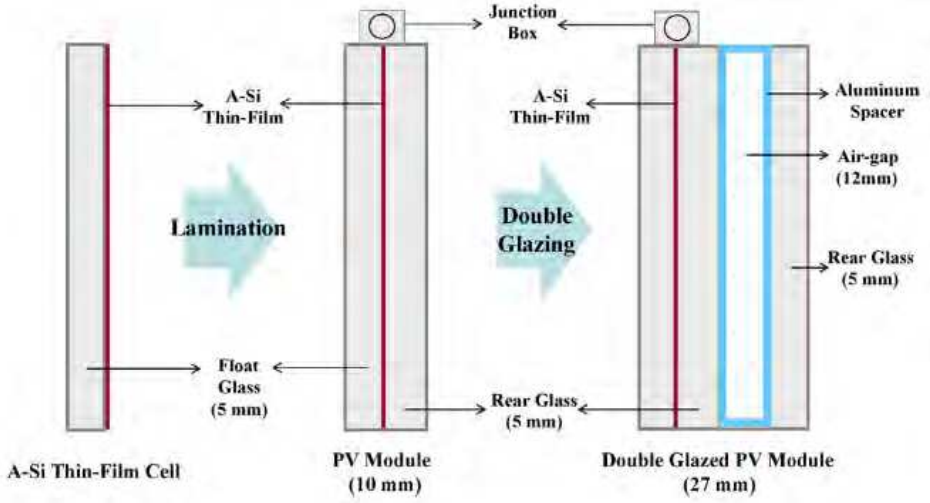

Fig. 2. Preparation for single plate of double-glazed PV module using transparent amorphous silicon (A-Si) thin-film cell.

From the performance evaluation of the heat insulation, the prepared PV module exhibited a 2.64 W/m^2-℃ thermal transmittance, as shown in Figure 3. However, it showed an 18 % solar heat gain coefficient (SHGC), which was much lower than that measured for the common double glazed window. WINDOW 6.0 and THERM5.0 (LBNL, USA) were used to analyze the heat insulation of the standard type of double glazed PV module widely used

for the heat insulation of building windows and doors. This analysis allowed for the evaluation of heat transfer under a two dimensional steady state for the user defined fitting system at a given circumstance.

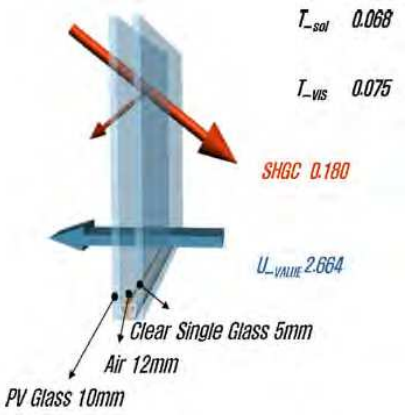

Fig. 3. Optical and thermal characteristics of double-glazed PV module (T_sol is the solar transmittance, T_vis is the transmittance of visible radiation, SHGC is the solar heat gain coefficient, and U_value is the thermal transmittance of PV module).module

Figure 4 shows a plane figure of a 10 mm thick and 980 × 950 mm single plate PV module, and a PV module consists of 108 cells in series. The electrical characteristics of the prepared PV module are listed in Table 1.

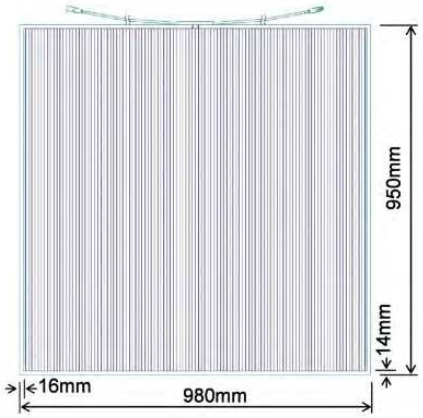

Fig. 4. Plane figure of a single plate PV module.

4. Full-scale mock-up model

A full-scale mock-up model was constructed with the dimensions of 8 m long, 5 m wide, and 3.5 m high, as shown in Figure 5. In order to demonstrate the impact of the inclined

Item	Specification
Module thickness (mm)	10
Module efficiency (%)	7
Maximum power output (W)	44.0
Maximum voltage (V)	59.6
Maximum electric current (A)	0.74
Open circuit voltage (V)	91.8
Short circuit current (A)	0.972

Table 1. Specification of the tested thin-film PV module

slope (incidence angle) on the power output, the inclined angles were varied on the mock-up by installing both a tilted roof at 30º and a common roof without any slope. The mock-up faced south in order to maintain a compatible solar irradiance with the location of Yongin, Gyeonggi, Korea. Two separated spaces were prepared in order to test the thin-film PV module (Test room A in Figure 5(a)) and the common double glazed window (Test room B in Figure 5(a)) as a reference. The spaces were 2 m long, 3 m wide, and 2.7 m high. The double glazed PV module and the common double-glazed window were installed in each separated test room at different inclined angles (0 º, 30 º, and 90 º).

A mock-up model was also constructed in order to monitor the electric current, voltage, power, temperature, and solar irradiation depending on the inclined angle of the PV module. The double glazed thin-film PV module revealed only a 10 % transmittance (See Figure 1), but this was as sufficient as the common double glazed window for observing the outside.

5. Power performance of PV module

5.1 PV module performance measured in mock-up model

The total solar irradiance and power output of the PV module, depending on the inclined angle of double glazing, were monitored through the mock-up model for 9 months from November 2006 to August 2007. Data obtained from the mock-up was collected based on minute-averaged data, and the final data of 12,254,312 was statistically analyzed based on 56 variables. Firstly, daily data was rearranged into monthly data. Secondly, minute-based data was averaged and combined into an hourly data. Finally, each group was analyzed in terms of an arithmetic mean, standard deviation, minimum, and maximum value. The empirical data in this study was limited in DC output, which was obtained from the load using resistance without an inverter. Thus, it is assumed that there may be a number of differences between the data measured in this study and the empirical data controlled by maximum power peak tracking (MPPT) using an inverter.

Figure 6 shows the hourly data, which was yearly-averaged, of the intensity of solar irradiance and DC output depending on the inclined angle of the double glazed PV module. Based on the data measured at noon, the inclined slope of 30 º (SLOPE _30) revealed an insolation of 528.4 W/m², which shows a greater solar irradiation than that for the slopes of 0 º (SLOPE_0, 459.6 W/m²) and 90 º (SLOPE_90, 385.0 W/m²), as shown in Figure 6(a). Consequently, the average power output at noon also exhibited 19.9 W for SLOPE_30, which was higher than that shown in the data for SLOPE_0 (15.76 W) and SLOPE_90 (8.6 W) (See Figure 6(b)).

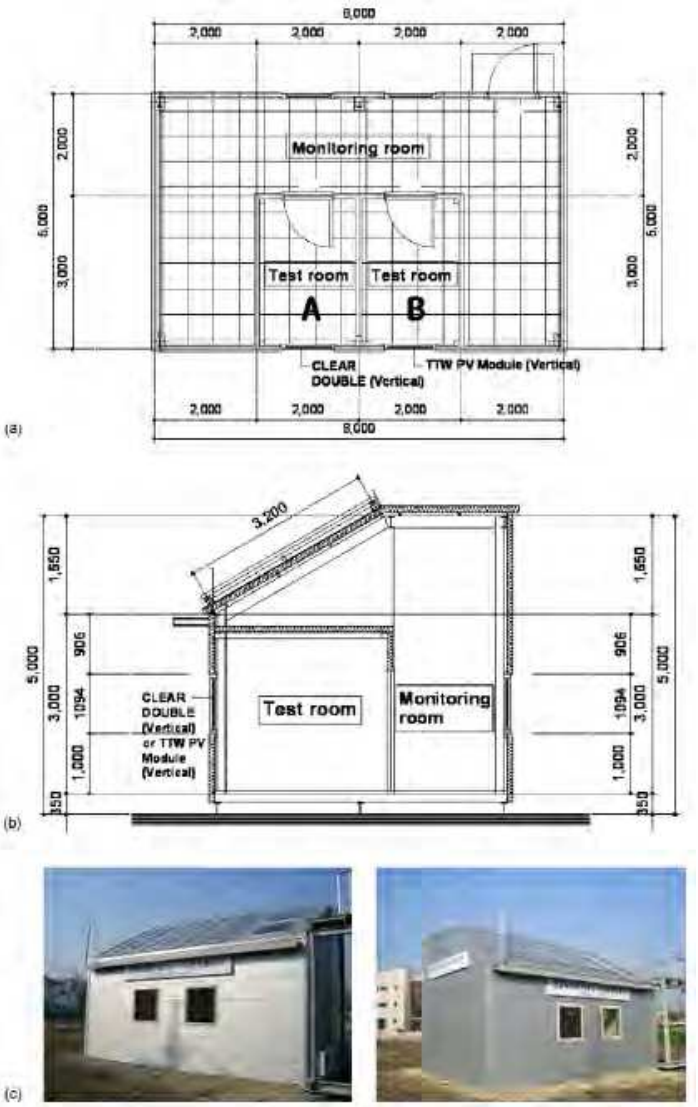

Fig. 5. Full-scale mock-up model: (a) a floor plan view, (b) a cross-sectional view, and (c) photographs of mock-up model.

5.2 Effect of intensity of solar irradiance

Figure 7 depicts the relationship between the solar irradiance taken from the PV module and the DC power output depending on the inclined angle of the module. For all PV modules, the power output increased with an increase in solar irradiance. While the increase rate of power output was particularly retarded under the lower solar irradiance, there was a very steep increase of power output under the higher solar irradiance (See Figure 7).

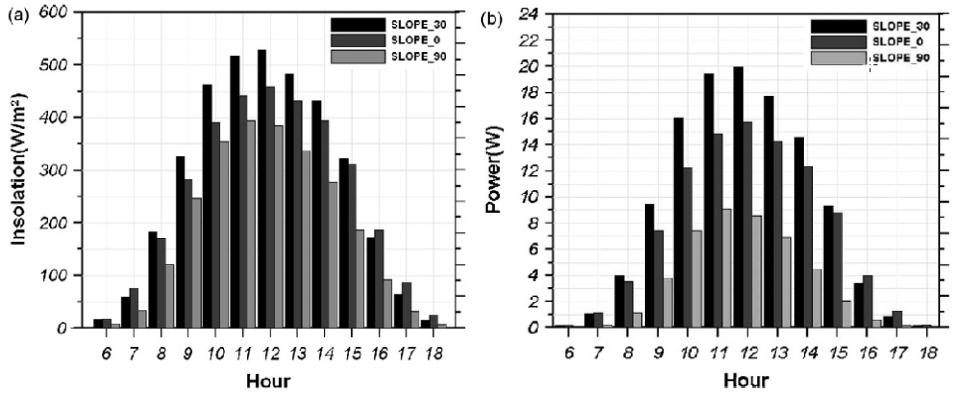

Fig. 6. Monitoring data of PV module depending on the slope through the mock-up model: hourly data averaged yearly: (a) solar irradiance and (b) power output.

By observing the degree of scattering for each inclined PV module as shown in Figure 7, there was a higher density of power output distribution for SLOPE_30 under the higher solar irradiance. On the other hand, the lowest distribution of power output was revealed for SLOPE_90, even under the higher solar irradiance. The monthly-based analysis revealed that a double glazed PV module inclined at 30 º (SLOPE_30) produced the greatest power output due to the acquisition of a higher solar irradiation. This result can also be achieved from a PV module with an incidence angle of 40.2 º, implying that it is more efficient to acquire solar irradiation than any other factor (See Figure 7(b)).

In the case of SLOPE_0, there were significant differences in power output with respect to solar irradiance depending on monthly variation (See Figure 7(a)). Specifically, the maximum solar irradiance in December is only 500 W/m² resulting in a power output of 10 W. On the other hand, the maximum solar irradiance of 1,000 W/m² with over 50 W power output was recorded for June. This high efficiency of power performance for SLOPE_0 during the summer could be due to the incidence angle of 36.1 º, which was low enough to absorb solar irradiation.

The reverse tendency of power output for SLOPE_0 was shown for SLOPE_90, which was installed at the horizontal plane. Specifically, a maximum power output of above 30 W was observed. This was due to a quiet efficient solar irradiance with the maximum solar irradiation gain of over 900 W/m² occurring in December. However, a lower solar irradiance of around 500 W/m² with less than 10 W power output was observed during the summer months from June to August. This can be explained by the difference in the incidence angle of the PV module depending on the inclined slope, i.e., the lower incidence angle of 36.6 º for SLOPE_90 was observed during the winter, particularly in January, while the higher value of 84.6 º was observed during the summer, especially in June. This implies that solar irradiation capable of producing a much higher power output can be easier to be achieved with a lower incidence angle of solar radiation to the PV module.

5.3 Monthly based analysis of power performance

Figure 8 shows the amount of solar irradiation and power output accumulated for each month depending on the inclined angle of the PV module. A fairly effective solar irradiance

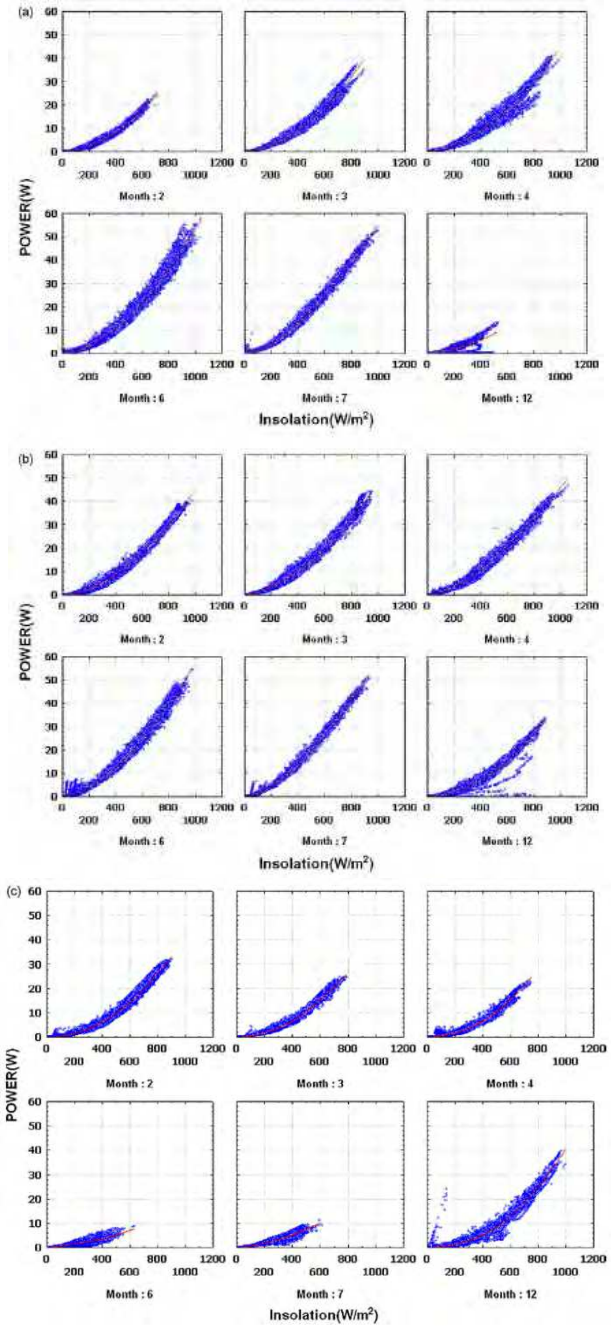

Fig. 7. Power output data of PV modules based on monthly variation of solar irradiance measured in the mock-up model: (a) slope 0, (b) slope 30, and (c) slope 90, respectively.

of 147.7 kWh/m² was obtained from SLOPE_30 during May, and the lowest value of 75.3 kWh/m² was obtained in December (See Figure 8(a)). The horizontal module of SLOPE_0 resulted in the highest solar irradiance in June and the lowest value in January. On the other hand, the PV module installed at the vertical window exhibited the highest solar irradiance (115 kWh/m²) in January and the lowest (50.2 kWh/m²) in August. This can be explained by the highly effective solar irradiance of both of the PV modules that were installed horizontally (SLOPE_0) and tilted at a slope of 30 °. This was due to the smaller incidence angle, defined as the angle between the incident solar ray and the normal line, close to the horizontal plane during the summer and related to the height of the sun, while the PV module installed vertically (SLOPE_90) obtained an effective solar irradiance due to the smaller incidence angle during the winter.

An analysis was also carried out on the monthly power performance depending on the inclined angle of the PV module, as shown in Figure 8(b). From the monthly data in Figure 8(b), it can be seen that the most effective power output during the summer, particularly for June, was obtained at SLOPE_30 and SLOPE_0. However, the highest power output was obtained at SLOPE_90 for January. This could be due to the variation of solar irradiance from each PV module from the different incidence angles based on the height of the sun.

In this study, the best power performance among all the tested PV modules was that obtained by the PV module tilted at an angle of 30 ° (SLOPE_30), comparing with those installed horizontally (SLOPE_0) and vertically (SLOPE_90).

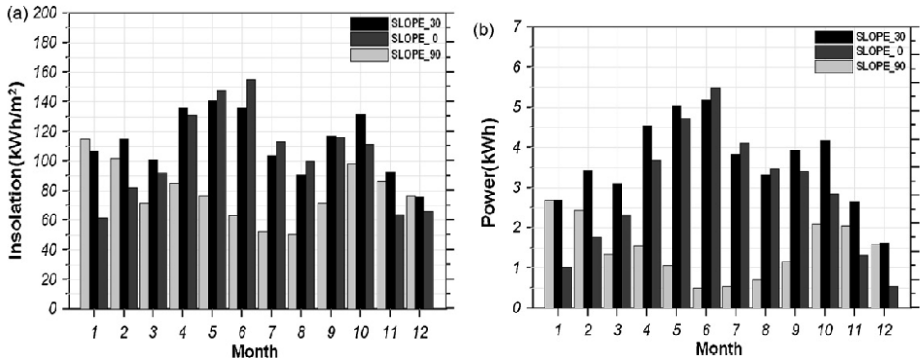

Fig. 8. Monitoring data of PV module depending upon the slope through the mockup model: monthly accumulated data of (a) solar irradiance and (b) power output.

5.4 Hourly based analysis of power performance

Figures 10~12 show the statistically analyzed monthly power generation data of PV module depending the inclined slope. The name of each part is provided for the better understanding in Figure 9. ■ sign in each box indicates Mean value, □ and ▨ signs indicate the range of Mean±S.D (Standard Deviation), Whisker Ⅰ sign indicates the range between maximum and minimum values. For example, in the first graph of Figure 10, the mean value at 12pm in January is approximately 20W, S.D. (Standard Deviation) is 5~30W, maximum value is 40W and the minimum value is 0W. The statistical data on how much power is generated in each hour can be easily understood with these graphs. Furthermore, the maximum and minimum ranges can also be easily analyzed, enabling the comparison of characteristic behaviors depending on the inclined angle.

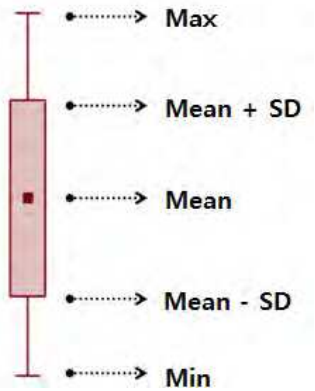

Fig. 9. Explanation of Box-Whisker graph

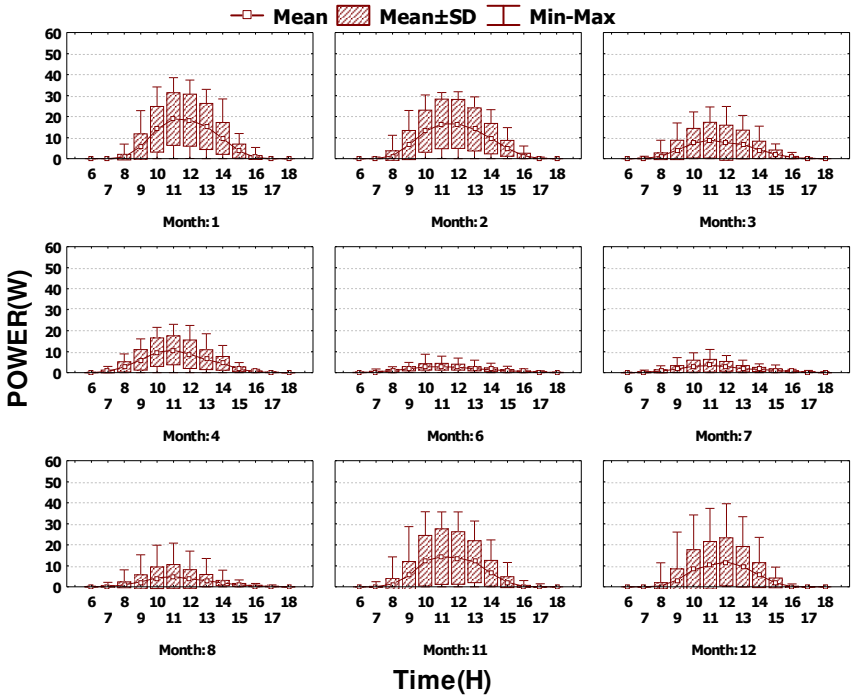

Fig. 10. Power generation of SLOPE._90° in each timestep

In case of vertical PV module, the power generation turns out be significant in Janurary due to a farily effective solar irradiance. It showed the power generation of 20W on average at noon. On the other hand, in June when there is no high solar irradiance due to high incidence angle, the power generation was less then 10W on average at noon. The inclined slope of 30 ° showed the best power generation during the measurement period. Especially the power generation was the greatest in June with 30W on average at noon.

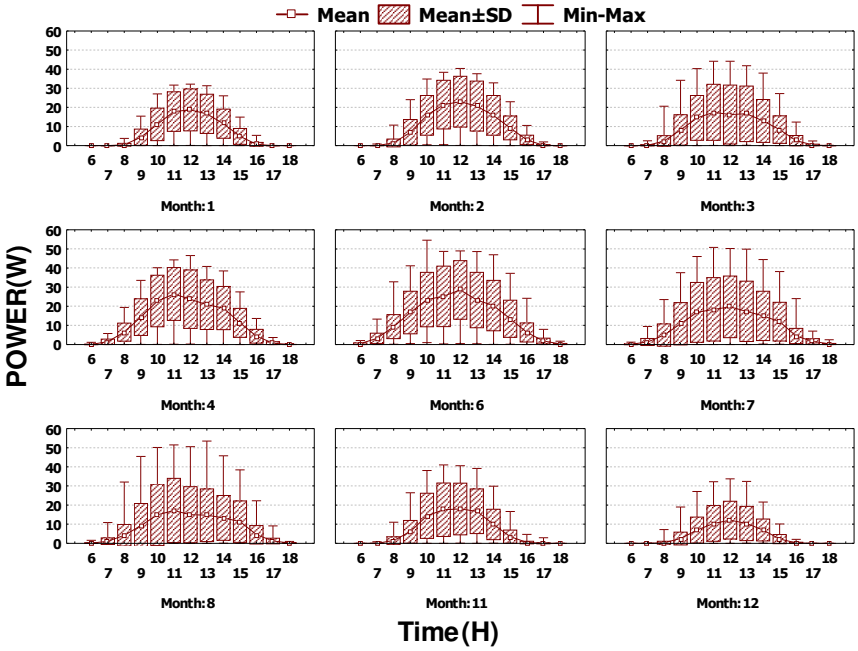

Fig. 11. Power generation of SLOPE._30° in each timestep

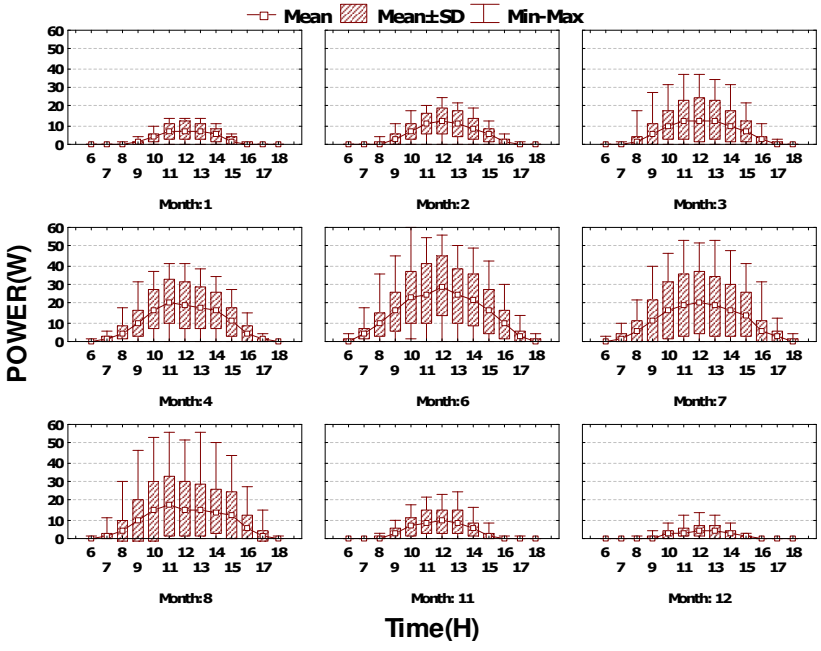

Fig. 12. Power generation of SLOPE._0° in each timestep

In case of horizontal PV module, it showed effective power generation performance in the summer similar to the case of the inclined slope of 30 °, showing more than 30W generation on average at noon. However, the generation barely exceeded 10W in December due to high incidence angle and low solar irradiance. The hourly average power generation depending on each inclined angle is illustrated in Figure 13. In case of inclined angle (SLOPE_30), it showed power generation of 20W on average at noon, while the horizontal PV module showed 15W on average. Vertical PV (SLOPE_90) showed the low generation performance of 8W on average. Table 5.5 summarizes the hourly average power generation, voltage and electric current.

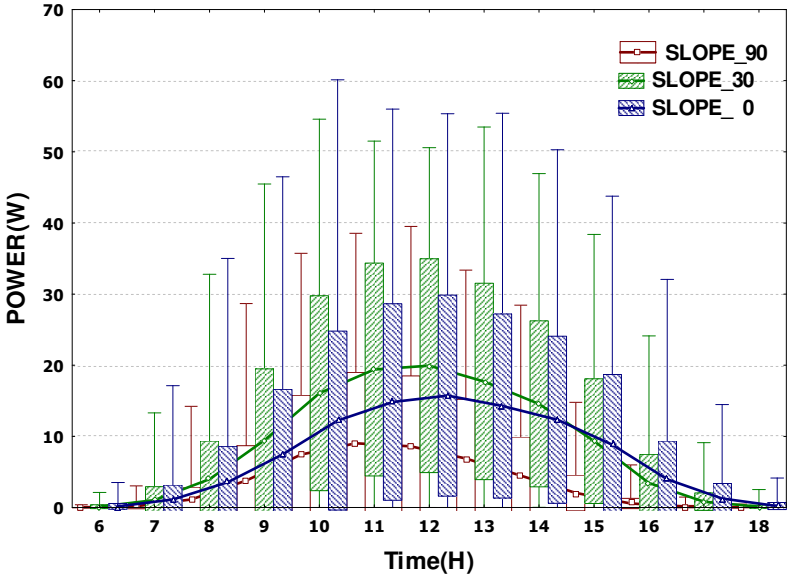

Fig. 13. Annual hourly averaged power generation

5.5 Analysis of power performance through simulation

In this study, TRNSYS (Ver. 14.2, Solar Energy Laboratory, Univ. of Wisconsin, USA) was used as a simulation program to analyze the performance of power output for a double glazed PV module. Generally, TRNSYS has been widely used to compute the hourly data for power output, solar irradiance, temperature, and wind speed for both PV systems and solar heat energy systems [10]. From the simulation program, the relative error was verified, and a comparison was then made of the power output from the experimental and the computed data, as shown in Figure 14. In addition, the experimental data from the PV module with an inclined angle of 30 ° (SLOPE_30) was compared with the simulated data in terms of the annual power output: 1,060 kWh/kWp was obtained from the experiment and 977 kWh/kWp was estimated from the computational simulation. This computed data showed a relative error of 8.5 %, which is considered to be a reliable result within the error tolerance. Thus, the computational simulation was conducted to demonstrate the power output performance of a PV module installed at various inclined angles.

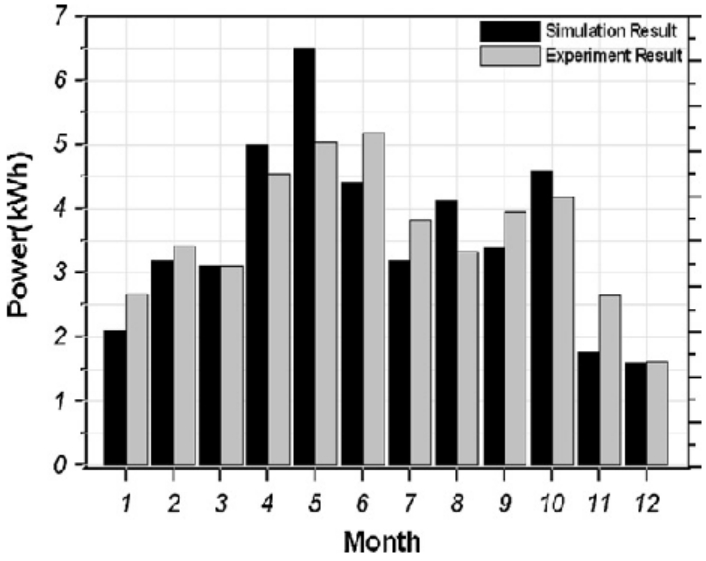

Fig. 14. Power output data calibration by comparing the experimental data to the computed data obtained from the simulation program (TRNSYS).

Power performance analyses were performed of PV modules facing south (azimuth = 0 º) depending on the different inclined angles of 0 º, 10 º, 30 º, 50 º, 70 º, and 90 º. The data set consisted of the experimental data for 0 º, 30 º, and 90 º and the computed data for 10 º, 50 º, and 70 º. Figure 15 illustrates the monthly power output depending on the inclined angle ranging from 0 º to 90 º south (azimuth = 0 º). PV modules that were tilted at an angle below 30 º showed a relatively good power performance of over 6 kWh in the summer, while those with an inclined angle above 50 º demonstrated a power performance of less than 6 kWh. The most effective annual power output data of 977 kWh/kWp was obtained at an inclined angle of 30 º (SLOPE_30), as shown in Figure 16. On the other hand, the lowest annual power output of 357 kWh/kWp was obtained from the PV module with a slope of 90 º (SLOPE_90), which was 37 % of the annual power output of SLOPE_30. From Figure 16, it can be seen that the annual power output performance was effective in the order of SLOPE_10 (954 kWh/kWp), SLOPE_0 (890 kWh/kWp), SLOPE_50 (860 kWh/kWp), and SLOPE_70 (633 kWh/kWp).

The power generation performance depending on the angle of the azimuth was also estimated for PV modules with different inclined slopes, as shown in Figure 17. Similarly, a PV module inclined at an angle of 30 º showed the most effective power output data for all directions in terms of azimuth angles, and the lowest data was obtained from that with an inclined angle of 90 º. For the PV module inclined at an angle of 30 º, the best power performance among the analyzed PV modules facing various directions was obtained for the PV module that was installed to the south (azimuth = 0 º). It can be seen from Figure 17 that different azimuth angles affected the power performance of PV modules: that is, the power performance decreased as the direction of the PV module was changed from the south to the east and west, in comparison to the PV modules that were inclined at the slope of 30 º, as listed in Table 2.

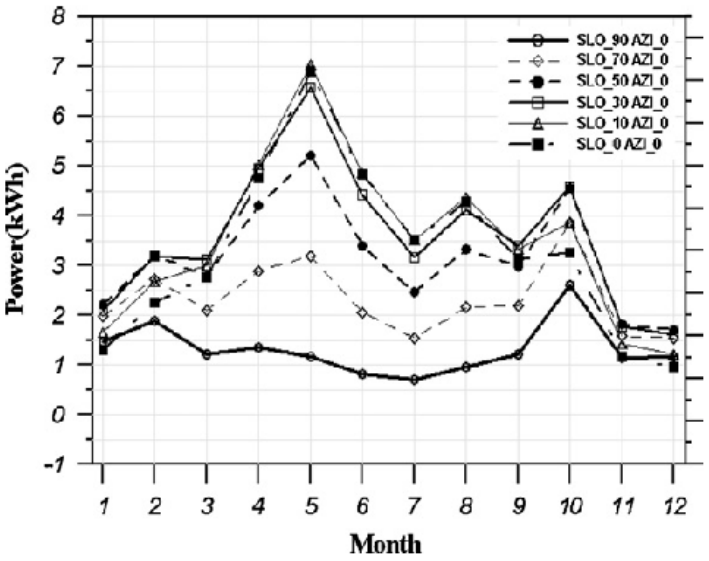

Fig. 15. Monthly power output data of PV module depending on the slope, and facing south (azimuth = 0).

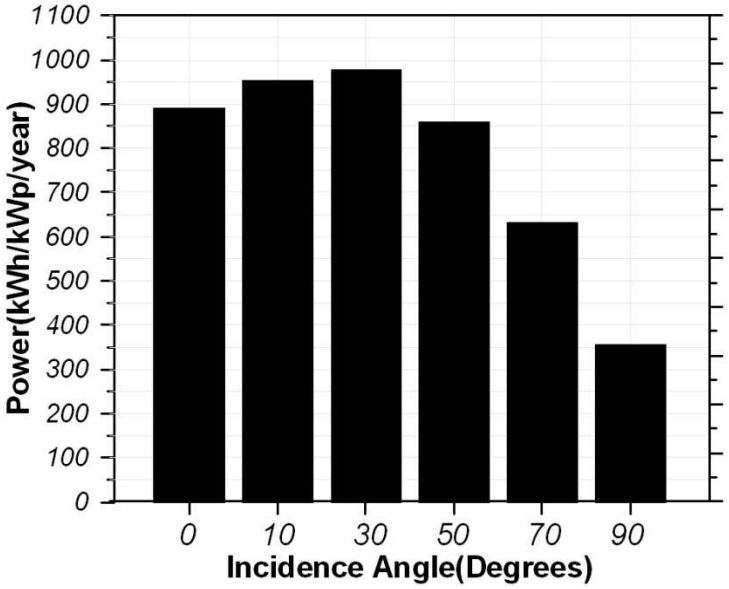

Fig. 16. Annual power production of PV module depending on the slope, and facing south (azimuth = 0).

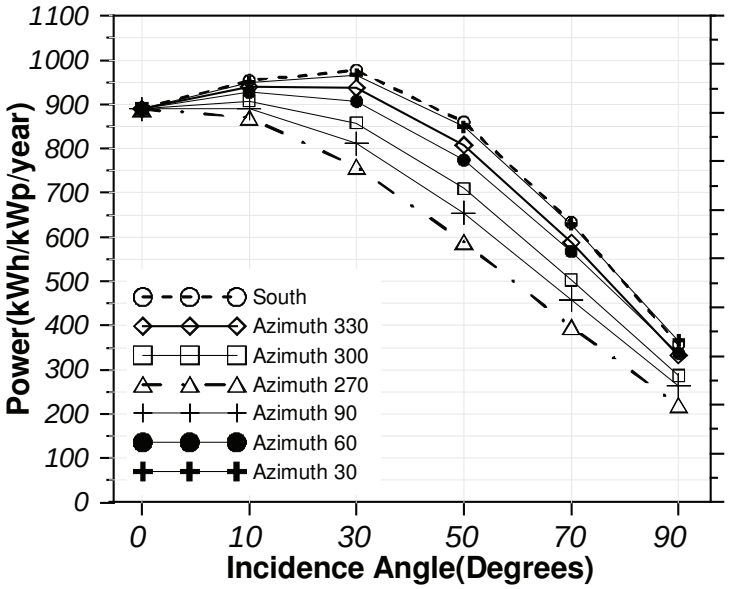

Fig. 17. Annual power production of PV modules with various slopes depending on the angle of azimuth ranging from 0 to 90

Angle of azimuth (°)	Direction	Power performance efficiency[a] (%)
0	South	100
30	Southwest 30 °	99
60	Southwest 60 °	93
90	West	83
270	East	78
300	Southeast 60 °	88
330	Southeast 30 °	96

a. Power performance efficiency was calculated from the percent of power output at each azimuth angle on the basis of the power output data of PV module to the south.

Table 2. Power performance efficiency of PV module with a slope of 308 depending on azimuth angle

It can be seen from Figure 17 that for the annual power performance of several PV modules, the power output increased with an increase of the inclined angle below 30 °, and decreased with an increase of the inclined angle above 30 °. In particular, at inclined slopes above 60 ° there was a steep decline of power performance with the increase of the inclined slope, as shown in Figure 17. This could be due to the incidence angle modifier correlation (IAM) of glass attached to the PV module, which showed a similar tendency in IAM depending on the inclined angle [11], as can be seen in Figure 18. Actually, IAM should be computed as a function of incidence angle (θ) when estimating the power output of the PV module, by using the following Equation (1) [11]:

$$IAM = 1 - (1.098x10^{-4})\theta - (6.267x10^{-6})\theta^2 + (6.583x10^{-7})\theta^3 - (1.4272x10^{-8})\theta^4 \quad (1)$$

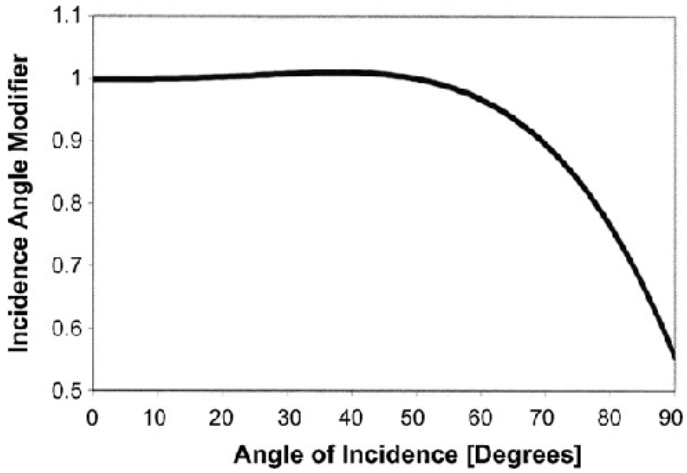

Fig. 18. Correlation of incidence angle modifier given by King et al. (1994).

Accordingly, a characteristic of the glass attached to the PV module is considerably influential so that the solar transmittance (Tsol) remarkably decreases with an increase in the inclined slope of the PV module from the higher incidence angle. Therefore, the solar transmittance efficiency can significantly affect the power output of the PV module.

6. Power efficiency of PV module

6.1 Hourly based analysis of the power efficiency

The power efficiency can be calculated by multiplying total irradiation by the PV window area. Annual averaged power efficiency is illustrated in Fig. 19.

$$\eta_{S,\tau} = \frac{E_{use,\tau}}{A_a \text{ X } H_\tau}$$

$\eta_{S,\tau}$; Power Efficiency
$E_{use,\tau}$; Power Output(Wh)
A_a ; PV windows area (m^2)
H_τ ; Total irradiation on the PV windows

Annual average power efficiencies of the inclined slope of 30 º (SLOPE_30), horizontal PV module (SLOPE_0) and vertical PV module (SLOPE_90) turned out to be 3.19%, 2.61% and 1.77%, respectively, indicating that the inclined slope of 30 º showed the greatest efficiency. On the other hand, the horizontal PV showed the highest instantaneous peak power efficiency of 6.0% followed by those of the inclined slope of 30 º (5.6%) and vertical PV (4.0%) angles. In terms of the monthly average power efficiency depending on each inclination angle, the inclined slope of 30 º (SLOPE_30) showed 3.82% in June and the horizontal PV (SLOPE_0) showed 3.63% in July. The inclined slope of 30 º showed 2.15 % of efficiency and the horizontal PV showed 0.81% in December. On the other hand, the vertical

PV (SLOPE_90) showed the peak efficiency of 2.38% in February and lowest efficiency of 0.80% in June. The inclined slope of 30 º (SLOPE_30) showed the greatest annual average power efficiency of 3.19%, followed by horizontal and vertical PV modules showing efficiencies of 2.61% and 1.77%, respectively.

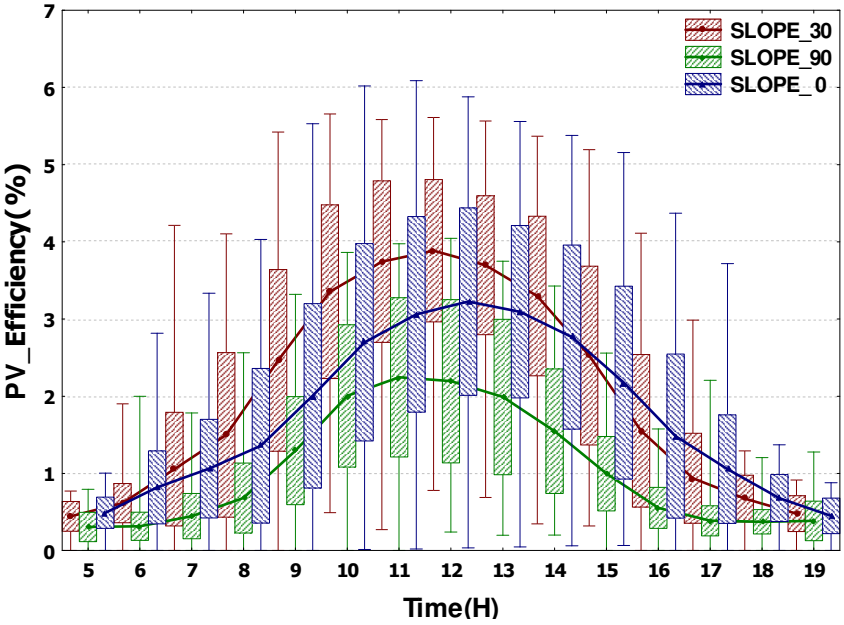

Fig. 19. Annual hourly averaged power efficiency

6.2 Effect of power efficiency by the intensity of solar irradiance

Assuming the solar irradiance of 900 W/m², the power efficiencies of the inclined slope of 30º and horizontal PV reached 5%, while the vertical PV partially exceeded 3%. The inclined slope of 30 º and horizontal PV showed relatively high power efficiency even under high solar irradiance conditions, while the efficiency of vertical PV significantly dropped after reaching 500W/m². The inclined slope of 30 º and horizontal PV can obtain relatively uniform solar irradiance throughout the year and thus the high power efficiency can be achieved over the large range of solar irradiance, while the vertical PV absorb the low solar irradiance during the winter period and thus the power efficiency is reduced in those low irradiance conditions.

6.3 Power efficiency by the temperature variation

The correlation between the power efficiency and the PV surface temperature variation is illustrated. Under the low solar irradiance, the data is scattered and thus did not show the clear correlation. However, it showed the clear correlation between PV efficiency and the surface temperature under the solar irradiance higher than 600W/m², i.e., the PV efficiency is improved at higher surface temperature. This is due to the fact that the higher surface temperature enhances the power efficiency in case of amorphous PV as opposed to crystalline silicon solar cell (c-Si solar cell).

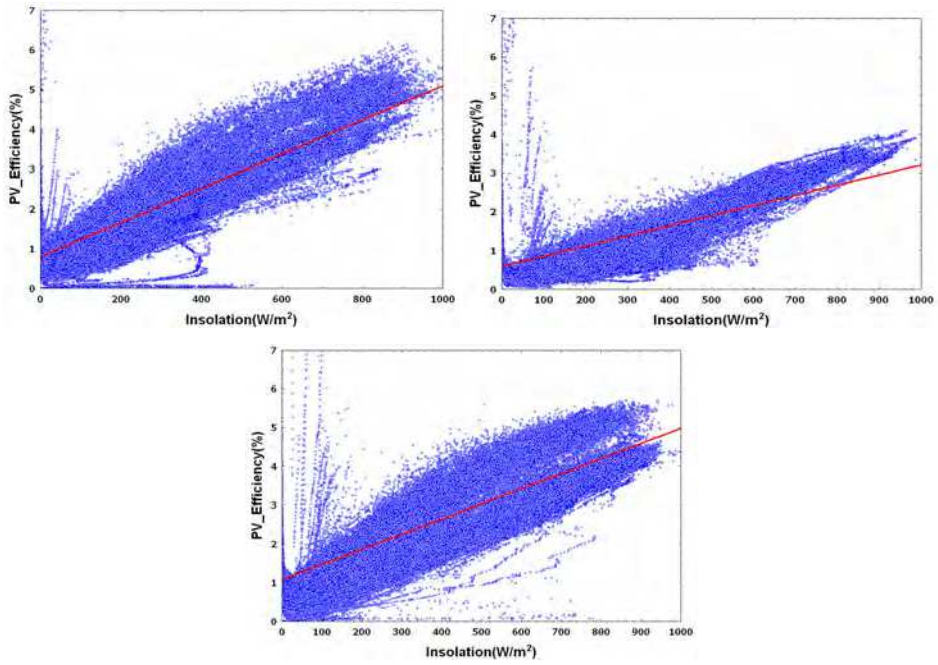

Fig. 20. Correlation between solar insolation and power efficiency (SLOPE_90°, SLOPE_30°, SLOPE_0°)

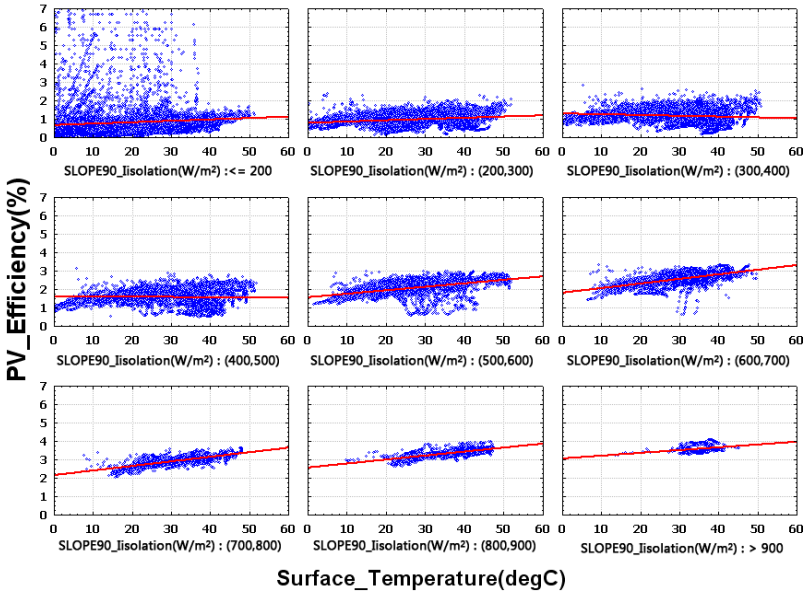

Fig. 21. Correlation between the surface temperature and power efficiency (SLOPE_90°)

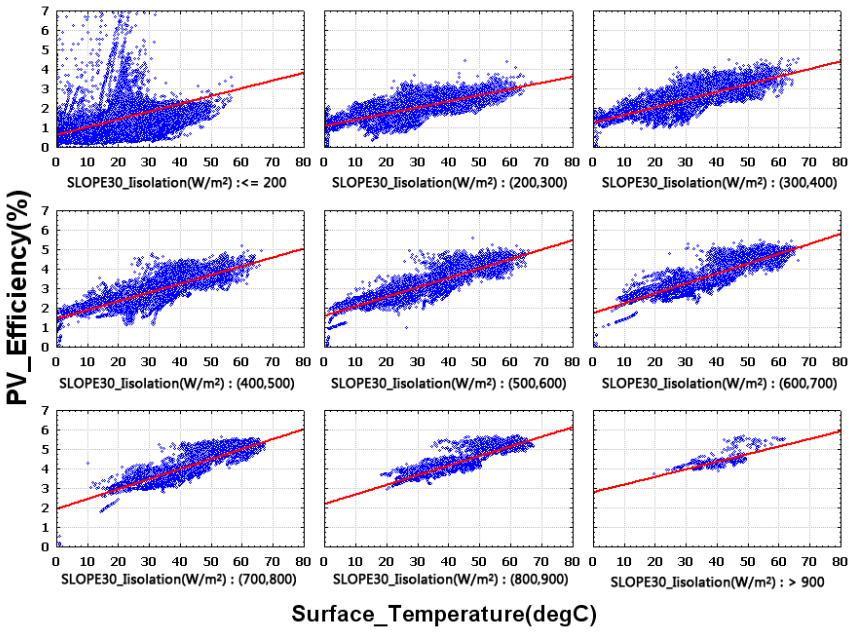

Fig. 22. Correlation between the surface temperature and power efficiency (SLOPE_30°)

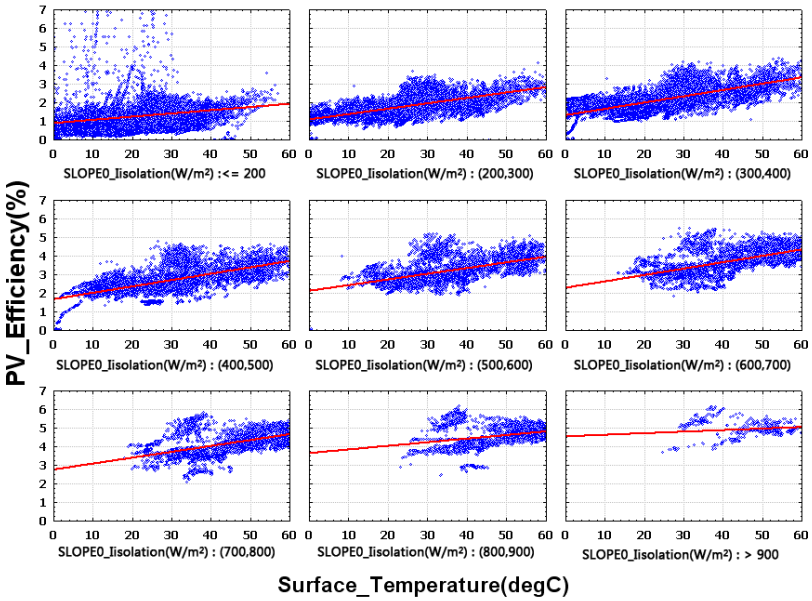

Fig. 23. Correlation between the surface temperature and power efficiency (SLOPE_0°)

6.4 Power efficiency by the solar incidence angle

The PV efficiencies of each inclination angle under different solar incidence angle and solar irradiance are illustrated in the figures below. In case of vertical PV module (SLOPE_90), the power efficiency showed constant value until the solar incidence angle of 65° and it started to rapidly drop after 65°. These characteristics are considered to be the effect of absorbed solar insolation (incident angle modifier) depending on the solar incidence angle reaching the PV module glass wall. This phenomenon did not take place in case of the inclined slope of 30 ° (SLOPE_30) due to the low PV efficiency at the solar incidence angle higher than 65°. Likewise, the horizontal PV module was not affected by incident angle modifier as well in most of the solar radiation conditions except for the high solar incidence angle of greater than 65° and the low solar insolation of less than 400W/m² where the efficiency was rather decreased.

It turns out that the power efficiency of PV module is largely affected by the solar incidence angle, solar azimuth and altitude. Furthermore, the rapid decrease in the PV efficiency during the summer period is due to the reduced solar transmittance through the window system at the solar incidence angle higher than 70°, showing the impact of the front glass of PV module on the power efficiency.

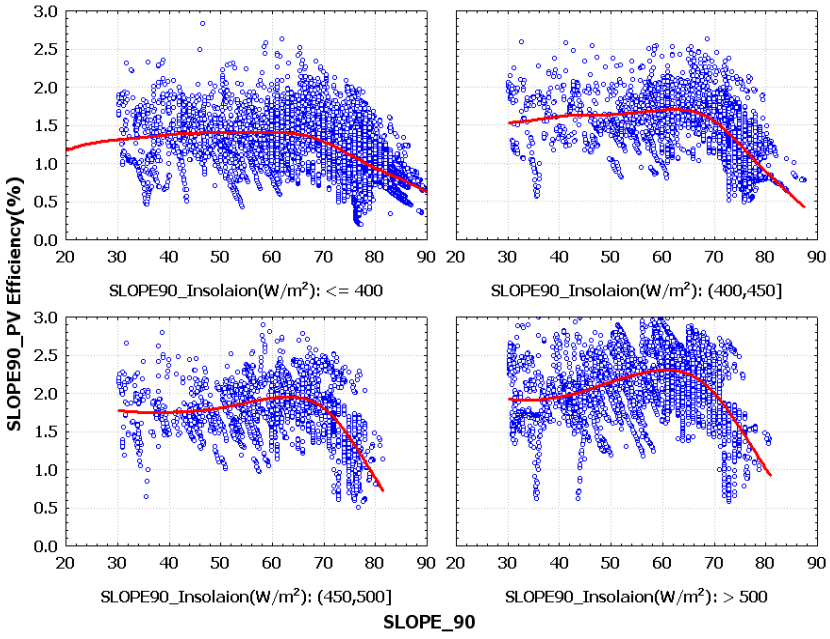

Fig. 24. PV module power efficiency vs. solar incidence angle (SLOPE_90°)

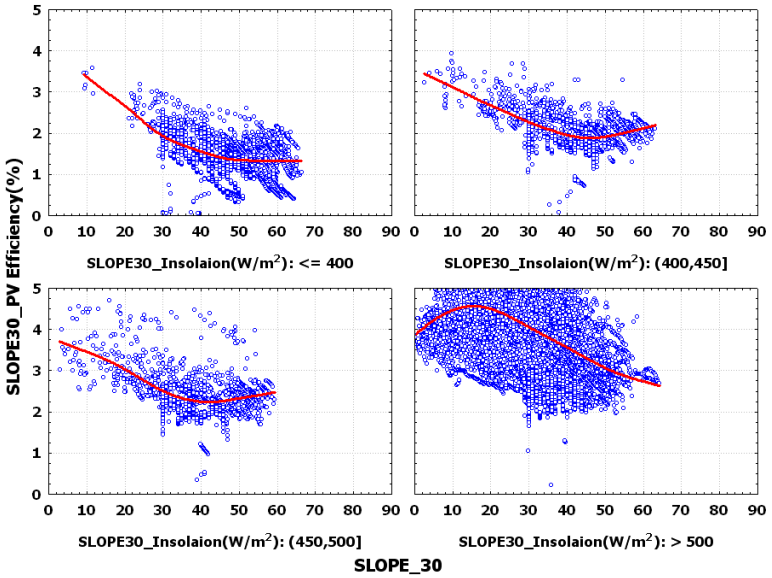

Fig. 25. PV module power efficiency vs. solar incidence angle (SLOPE_30°)

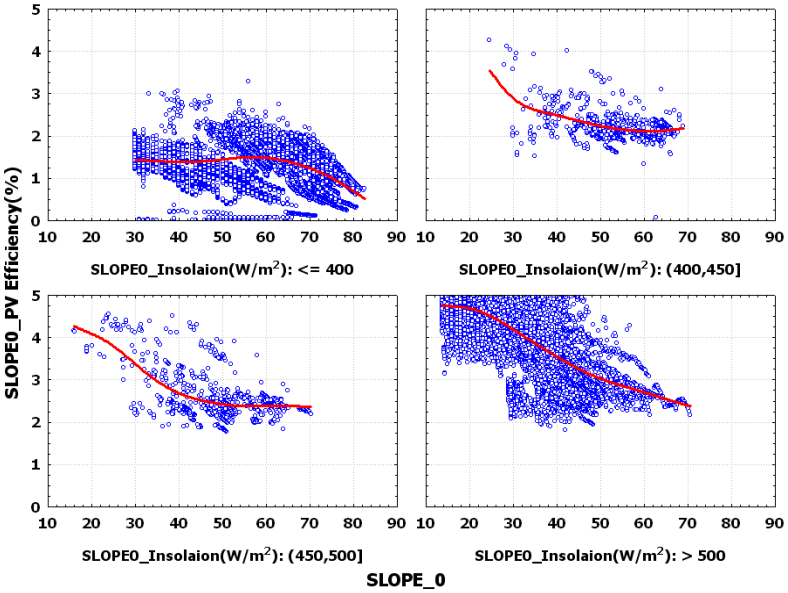

Fig. 26. PV module power efficiency vs. solar incidence angle (SLOPE_0°)

7. Conclusion

This study evaluated a transparent PV module in terms of power generation performance depending on installation conditions such as the inclined slope (incidence angle) and the azimuth angle. The objective of this evaluation was to provide useful data for the replacement of traditional building windows by BIPV system, through the experimental results measured in the full-scale mock-up system.

1. The annual power output of the PV module was measured through the mock-up model. The PV module that was installed at a slope of 30 º exhibited a better performance of 844.4 kWh/kWp annual power output than the vertical PV module with a slope of 90 º.
2. The experimental data was compared with the computed data obtained from the simulation program. The computed data is considered to be reliable with a relative error of 8.5 %. The best performance of annual power output was obtained from the PV module with a slope of 30 º facing south, at an azimuth angle of 0 º. The inclined angle was one of the factors that significantly influenced the power generation performance of the PV module, which varied within a range of 24 % on average and provided a maximum difference of 63% in the power output at the same azimuth angle.
3. In terms of the computed power output from a slope of 30 º depending on the azimuth angle, the PV module facing south exhibited the most effective performance compared to other azimuth angles. The direction in which the PV module faces can also be a very important factor that can affect the power performance efficiency by 11 % on average and by a maximum of 22 %, depending on the azimuth angle.

8. References

[1] Y. Kuwano, Progress of photovoltaic system for houses and buildings in Japan, Renewable Energy 15 (1998) 535–540.

[2] A. Ja¨ger-Waldau, Photovoltaics and renewable energies in Europe, Renewable and Sustainable Energy Reviews 11 (2007) 1414–1437.

[3] A. Stoppato, Life cycle assessment of photovoltaic electricity generation, Energy 33 (2008) 224–232.

[4] A. Hepbasli, A key review on exergetic analysis and assessment of renewable energy resources for a sustainable future, Renewable and Sustainable Energy Reviews 12 (2008) 593–661.

[5] A. Zahedi, Solar photovoltaic (PV) energy; latest developments in the building integrated and hybrid PV systems, Renewable Energy 31 (2006) 711–718.

[6] S. Teske, A. Zervos, O. Schafer, Energy revolution, Greenpeace International, European Renewable Energy Council (EREC) (2007).

[7] R.W. Miles, G. Zoppi, I. Forbes, Inorganic photovoltaic cells, Materials Today 10 (2007) 20–27.

[8] S. Guha, Amorphous silicon alloy photovoltaic technology and applications, Renewable Energy 15 (1998) 189–194.

[9] J.H. Song, Y.S. An, S.G. Kim, S,J. Lee, Jong-Ho Yoon, Y.K. Choung, Power output analysis of transparent thin-film module in building integrated photovoltaic system(BIPV), Energy and Building, Volume 40, Issue 11, (2008) 2067-2075

[10] TRNSYS, A transient system simulation program version 14.2 Manual. Solar Energy Laboratory: University of Wisconsin, Madison, USA, 2000.

[11] D.L. King, et al., Measuring the solar spectral and angle of incidence effects on photovoltaic modules and irradiance sensors, in: Proceedings of the IEEE Photovoltaic Specialists Conference, 1994, pp. 1113–1116.

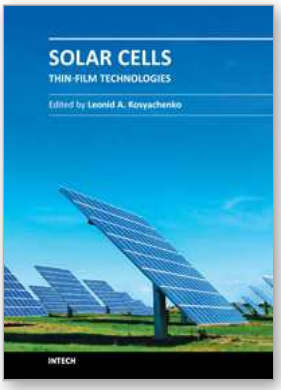

Solar Cells - Thin-Film Technologies

Edited by Prof. Leonid A. Kosyachenko

ISBN 978-953-307-570-9
Hard cover, 456 pages
Publisher InTech
Published online 02, November, 2011
Published in print edition November, 2011

The first book of this four-volume edition is dedicated to one of the most promising areas of photovoltaics, which has already reached a large-scale production of the second-generation thin-film solar modules and has resulted in building the powerful solar plants in several countries around the world. Thin-film technologies using direct-gap semiconductors such as CIGS and CdTe offer the lowest manufacturing costs and are becoming more prevalent in the industry allowing to improve manufacturability of the production at significantly larger scales than for wafer or ribbon Si modules. It is only a matter of time before thin films like CIGS and CdTe will replace wafer-based silicon solar cells as the dominant photovoltaic technology. Photoelectric efficiency of thin-film solar modules is still far from the theoretical limit. The scientific and technological problems of increasing this key parameter of the solar cell are discussed in several chapters of this volume.

InTech Europe
University Campus STeP Ri
Slavka Krautzeka 83/A
51000 Rijeka, Croatia
Phone: +385 (51) 770 447
Fax: +385 (51) 686 166
www.intechopen.com

InTech China
Unit 405, Office Block, Hotel Equatorial Shanghai
No.65, Yan An Road (West), Shanghai, 200040, China
中国上海市延安西路65号上海国际贵都大饭店办公楼405单元
Phone: +86-21-62489820
Fax: +86-21-62489821